Published for SISSA by Springer

Received: January 21, 2019
Revised: March 26, 2019
Accepted: April 7, 2019
Published: April 10, 2019

Observation of the doubly Cabibbo-suppressed decay $\Xi_c^+ \to p\phi$

The LHCb collaboration

E-mail: adzyuba@cern.ch

Abstract: The doubly Cabibbo-suppressed decay $\Xi_c^+ \to p\phi$ with $\phi \to K^+K^-$ is observed for the first time, with a statistical significance of more than fifteen standard deviations. The data sample used in this analysis corresponds to an integrated luminosity of $2\,\mathrm{fb}^{-1}$ recorded with the LHCb detector in pp collisions at a centre-of-mass energy of 8 TeV. The ratio of branching fractions between the decay $\Xi_c^+ \to p\phi$ and the singly Cabibbo-suppressed decay $\Xi_c^+ \to pK^-\pi^+$ is measured to be

$$\frac{\mathcal{B}(\Xi_c^+ \to p\phi)}{\mathcal{B}(\Xi_c^+ \to pK^-\pi^+)} = (19.8 \pm 0.7 \pm 0.9 \pm 0.2) \times 10^{-3},$$

where the first uncertainty is statistical, the second systematic and the third due to the knowledge of the $\phi \to K^+K^-$ branching fraction.

Keywords: Flavor physics, Branching fraction, Charm physics, Hadron-Hadron scattering (experiments)

ArXiv ePrint: 1901.06222

This paper is dedicated to the memory of our friend and colleague Yury Shcheglov.

https://doi.org/10.1007/JHEP04(2019)084

JHEP04(2019)084

Contents

JHEP04(2019)084

1 Introduction

The flavour structure of the weak interaction between quarks is described by the Cabibbo-Kobayashi-Maskawa (CKM) matrix [1, 2]. In particular, the tree-level decays of charmed particles depend on the matrix elements V_{ud}, V_{us}, V_{cd} and V_{cs}. The hierarchy of the CKM matrix elements becomes evident using the approximate Wolfenstein parametrisation, which is based on the expansion in powers of the small parameter $\lambda \approx 0.23$ with $|V_{ud}| \approx |V_{cs}| \approx 1 - \lambda^2/2$ and $|V_{us}| \approx |V_{cd}| \approx \lambda$ [3, 4]. Tree-level decays depending on both V_{us} and V_{cd} matrix elements are known as doubly Cabibbo-suppressed (DCS) decays. They have small branching fractions compared to the Cabibbo-favoured (CF) and the singly Cabibbo-suppressed (SCS) decays [5]. A systematic study of the relative contributions of DCS and CF diagrams to decays of charm baryons could shed light onto the role of the nonspectator quark, and in particular Pauli interference [6]. Such studies would be helpful for a better understanding of the lifetime hierarchy of charm baryons [6–9]. So far only one DCS charm-baryon decay, $\Lambda_c^+ \to pK^+\pi^-$, has been observed [10, 11].

This article reports the first observation of the DCS decay $\Xi_c^+ \to p\phi$ with $\phi \to K^+K^-$, hereafter referred to as the signal decay channel.[1] The leading-order diagram for the $\Xi_c^+ \to p\phi$ decay is shown in figure 1. The branching fraction of the signal decay channel is measured relative to the branching fraction of the SCS decay channel $\Xi_c^+ \to pK^-\pi^+$,

$$R_{p\phi} \equiv \frac{\mathcal{B}(\Xi_c^+ \to p\phi)}{\mathcal{B}(\Xi_c^+ \to pK^-\pi^+)} \,. \tag{1.1}$$

[1] The inclusion of charge-conjugated processes is implied throughout this article.

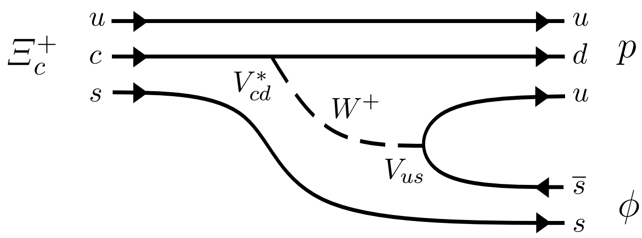

Figure 1. Tree quark diagram for the $\Xi_c^+ \to p\phi$ decay.

The measurement is based on a data sample of pp collisions collected in 2012 with the LHCb detector at the centre-of-mass energy of 8 TeV, corresponding to an integrated luminosity of $2\,\mathrm{fb}^{-1}$.

2 Detector and simulation

The LHCb detector [12, 13] is a single-arm forward spectrometer covering the pseudorapidity range $2 < \eta < 5$, designed for the study of particles containing b or c quarks. The detector includes a high-precision tracking system consisting of a silicon-strip vertex detector surrounding the pp interaction region [14], a large-area silicon-strip detector located upstream of a dipole magnet with a bending power of about 4 Tm, and three stations of silicon-strip detectors and straw drift tubes [15] placed downstream of the magnet. The tracking system provides a measurement of the momentum, p, of charged particles with a relative uncertainty that varies from 0.5% at low momentum to 1.0% at 200 GeV/c. The minimum distance of a track to a primary vertex (PV), the impact parameter (IP), is measured with a resolution of $(15 + 29/p_\mathrm{T})\,\mu\mathrm{m}$, where p_T is the component of the momentum transverse to the beam, in GeV/c. Different types of charged hadrons are distinguished using information from two ring-imaging Cherenkov detectors [16]. Photons, electrons, and hadrons are identified by a system consisting of scintillating-pad and preshower detectors, an electromagnetic and a hadronic calorimeter. Muons are identified by a system composed of alternating layers of iron and multiwire proportional chambers [17]. The online event selection is performed by a trigger [18], which consists of a hardware stage, based on information from the calorimeter and the muon systems, followed by a software stage, which applies a full event reconstruction.

At the hardware trigger stage, the events are required to have a muon with high p_T or a hadron, photon or electron with high transverse energy in the calorimeters. The software trigger requires a two-, three- or four-track secondary vertex with a significant displacement from any primary pp interaction vertex. At least one charged particle must have a transverse momentum $p_\mathrm{T} > 1.6$ GeV/c and be inconsistent with originating from any PV.

Simulation is used to evaluate detection efficiencies for the signal and the normalisation decay channels. In the simulation, pp collisions are generated using PYTHIA [19, 20] with the specific LHCb configuration [21]. Decays of hadronic particles are described by

JHEP04(2019)084

EvtGen [22], in which the final-state radiation is generated using Photos [23]. The interaction of the generated particles with the detector and its response are implemented using the Geant4 toolkit [24, 25] as described in ref. [26].

3 Selection of candidates

The candidates for the $\Xi_c^+ \to pK^-h^+$ decays, where $h^+ = \{\pi^+, K^+\}$, are formed using three charged tracks with $p_\mathrm{T} > 250\,\mathrm{MeV}/c$. Hadrons used for the reconstruction of the Ξ_c^+ baryons should not be produced at the PV. Only pions, protons, and kaons with an impact parameter χ^2_IP in excess of 9 with respect to all reconstructed PVs are taken into consideration for subsequent analysis. The χ^2_IP quantity is calculated as the difference in χ^2 of the PV fit with and without the particle in question. The momenta of the reconstructed final-state particles are required to be in the range 3.2–150 GeV/c for the mesons, and in the range 10–100 GeV/c for the proton. The reconstructed tracks must pass particle-identification (PID) requirements based on information from the RICH detectors, the calorimeter, and the muon stations [27]. The PID requirements are loose for mesons and much tighter for protons, to suppress π^+ and K^+ misidentified as protons. The three tracks must form a common vertex. The selected Ξ_c^+ candidates must have the rapidity (y) and transverse momentum $2.0 < y < 4.5$ and $4 < p_\mathrm{T} < 16\,\mathrm{GeV}/c$.

Additional requirements are introduced to suppress the contribution from D^+ and D_s^+ decays with pions or kaons misidentified as protons. Such background manifests itself as narrow peaking structures in the mass spectrum of the three hadrons if the mass hypothesis for the track identified as a proton is changed to a pion or kaon. Candidates with a mass within $\pm 10\,\mathrm{MeV}/c^2$ (approximately $\pm 2.5\sigma$) of the known values are rejected.

The average number of visible interactions per beam-crossing is 1.7 [13]. The candidate is associated to the PV with the smallest value of χ^2_IP. In order to evaluate the candidate Ξ_c^+ decay time and the two-body masses for the particles in the final state, a constrained fit is performed, requiring the Ξ_c^+ candidate to have originated from its associated PV and have a mass equal to its known value [28]. The proper decay time is required to be between 0.55 and 1.5 ps to reduce the fraction of baryons coming from b-hadron decays. The b-hadron component is also suppressed by the requirement on the χ^2_IP value of the reconstructed baryon to be less than 32. The masses of the pK^-h^+ combinations are calculated without the mass constraint. They are required to be in the range 2.42 to 2.51 GeV/c^2 for the Ξ_c^+ candidates.

In the offline selection, trigger objects are associated with reconstructed particles [18]. Selection requirements can therefore be made on the trigger selection itself and on whether the decision was due to the signal decay candidate (Trigger On Signal, TOS category), or to other particles produced in the pp collision (Trigger Independent of Signal, TIS category) or to a combination of both. The selected candidates must belong to the TIS category of the hardware-trigger and to the TOS category of the two levels of the software-trigger.

Only $\Xi_c^+ \to pK^-K^+$ candidates from the $\phi \to K^+K^-$ region, *i.e.* candidates with a K^-K^+ mass ($M_{K^-K^+}$) less than 1.07 GeV/c^2, are used. A very small fraction of $\Xi_c^+ \to p\phi$ events leaks into the $M_{K^-K^+} > 1.07\,\mathrm{GeV}/c^2$ region. In the $R_{p\phi}$ measurement this effect is taken into account using the distribution observed in simulated events. Figures 2 (left) and 3 show the mass distribution of the selected candidates for the $\Xi_c^+ \to pK^-K^+$ and $\Xi_c^+ \to pK^-\pi^+$ decay channels, respectively. Clear peaks can be seen in both distributions. The studies of the underlying background events suggest no peaking contributions for the signal and normalisation decay channels.

In parallel to Ξ_c^+ selections, samples of $\Lambda_c^+ \to pK^-h^+$ decays are also selected. The candidates for the Λ_c^+ decays are used to calibrate resolutions and trigger efficiencies and to perform other cross-checks.

4 Fit model and yields of signal and normalisation candidates

The yields of the selected $\Xi_c^+ \to pK^-h^+$ decays are determined from unbinned extended maximum-likelihood fits to the corresponding pK^-K^+ or $pK^-\pi^+$ mass spectra. The probability density function consists of a Gaussian core and exponential tails. The following distribution is used as the Ξ_c^+ model:

$$f_{\Xi_c^+}(x,\beta) \propto \exp\left\{\beta^2 - \sqrt{\beta^4 + x^2\beta^2}\right\}, \quad x = \frac{M-\mu}{\sigma(1+\epsilon\kappa)}, \tag{4.1}$$

where M is the candidate mass, μ is the peak position, σ reflects the core-peak width, κ is an asymmetry parameter, and β characterises the exponential tails [29]. The value of ϵ is -1 for $M \leq \mu$ and $+1$ for $M > \mu$. The parameter β is fixed in the fit of the $\Xi_c^+ \to pK^-K^+$ mass distribution to the value obtained from the fits of the normalisation and of the $\Lambda_c^+ \to pK^-K^+$ decay channels. The background is modelled by an exponential function. The results of the fits for the $\Xi_c^+ \to pK^-K^+$ and $\Xi_c^+ \to pK^-\pi^+$ decay channels are presented in figures 2 and 3, respectively. The yields are $N_{pKK} = 3790 \pm 120$ for the $\Xi_c^+ \to pK^-K^+$ decay channel and $N_{pK\pi} = (324.7 \pm 0.8) \times 10^3$ for the normalisation decay channel.

To separate the ϕ and non-ϕ contributions to the signal decay channel, the background subtracted K^-K^+ mass distribution is analysed. The subtraction is done using the *sPlot* technique [30]. The $M_{K^-K^+}$ observable is evaluated with the Ξ_c^+ mass constraint and is almost independent from the $M_{pK^-K^+}$ discriminating variable. The effect of the correlation is small and is taken into account in the systematic uncertainty of the measurement.

The fraction of the ϕ contribution (f_ϕ) in the selected $\Xi_c^+ \to pK^-K^+$ candidates is determined by a binned nonextended maximum-likelihood fit to the $M_{K^-K^+}$ spectrum. A P-wave relativistic Breit-Wigner distribution with Blatt-Weisskopf form factor [31] is used to describe the $\phi \to K^+K^-$ lineshape. The barrier radius is set to $3.5\,\mathrm{GeV}^{-1}$ in natural units. This distribution is convolved with a Gaussian function to model the experimental resolution. The parameters of the resolution function are fixed using the $\Lambda_c^+ \to pK^-K^+$ sample. For the non-ϕ contribution, the Flatté parameterisation [32] is used in the form

$$f_{\text{non-}\phi} \propto \left\{m_0^2 - M_{K^-K^+}^2 - im_0\left(g_1\rho_{\pi\pi} + g_2\rho_{KK}\right)\right\}^{-2}, \tag{4.2}$$

where m_0 refers to the mass of the $f_0(980)$ resonance, g_1 and g_2 are coupling constants, and $\rho_{\pi\pi}$ and ρ_{KK} are the Lorentz-invariant phase-space factors. The term $g_2\rho_{KK}$ accounts for the opening of the kaon threshold. The values $m_0 g_1 = 0.165 \pm 0.018\,\mathrm{GeV}^2$ and $g_2/g_1 =$

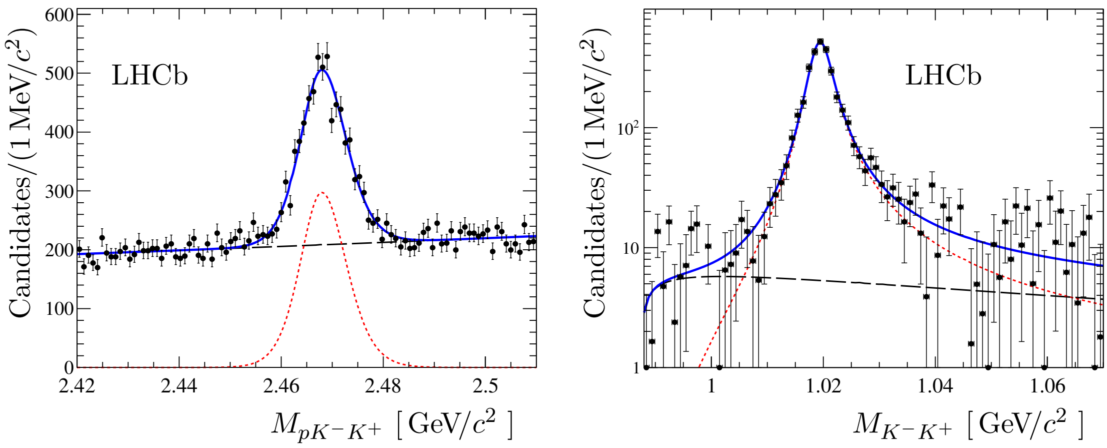

Figure 2. (Left) Fit results for the $\Xi_c^+ \to pK^-K^+$ decay. The candidates are selected in the ϕ meson region, *i.e.* with the requirement of $M_{K^-K^+} < 1.07\,\mathrm{GeV}/c^2$. The red dotted line corresponds to the signal component, the black dashed line reflects the background distribution, and the blue solid line is their sum. (Right) Background subtracted K^-K^+ mass distribution for the $\Xi_c^+ \to pK^-K^+$ decay. The red dotted line shows the $\Xi_c^+ \to p\phi$ contribution, the black dashed line represents the non-ϕ contribution, and the solid blue line is the total fit function.

4.21 ± 0.33 have been determined by the BES collaboration [33]. The choice of the Flatté parametrisation is suggested by the K^-K^+ mass distribution in the $\Lambda_c^+ \to pK^-K^+$ data sample. The ϕ contribution dominates in the K^-K^+ mass spectrum with a measured fraction $f_\phi = (90.0 \pm 2.7)\%$. The reported statistical uncertainty of the f_ϕ parameter is determined by a set of the pseudoexperiments, in which toy samples are generated according to result obtained for the alternative two-dimensional ($M_{pK^-K^+}$ vs. $M_{K^-K^+}$) model described below.

As a cross-check of the result obtained with the *sPlot* approach, an extended two-dimensional likelihood fit to the $M_{pK^-K^+}$ and $M_{K^-K^+}$ distributions is performed. Four two-dimensional terms are considered. The $M_{pK^-K^+}$ dependency for the ϕ and non-ϕ terms for the Ξ_c^+ decay component are described by eq. (4.1). Two additional ϕ and non-ϕ terms are introduced for the $M_{pK^-K^+}$ background description. These terms are independent linear distributions in the $M_{pK^-K^+}$ spectrum. A second-order polynomial is used to describe the K^-K^+ mass distribution of the non-Ξ_c^+ non-ϕ background. The results of the two-dimensional fit are in agreement with the *sPlot*-based procedure.

The statistical significance of the observation of the $\Xi_c^+ \to p\phi$ decay is estimated using Wilks' theorem [34] and is well above 15σ. The fit to the $M_{K^-K^+}$ distribution results in an evidence of a non-ϕ contribution to the DCS $\Xi_c^+ \to pK^-K^+$ decay. A statistical significance of 3.9σ is obtained under the assumption of normal distributions for the uncertainties.

5 Efficiencies and branching fractions ratio

The total detection efficiencies for both the signal and the normalisation decays can be factorised as

$$\epsilon_{\text{total}} = \epsilon_{\text{acc}} \times \epsilon_{\text{rec\&sel|acc}} \times \epsilon_{\text{software|rec\&sel}} \times \epsilon_{\text{hardware|software}} \times \epsilon_{\text{PID}}, \tag{5.1}$$

JHEP04(2019)084

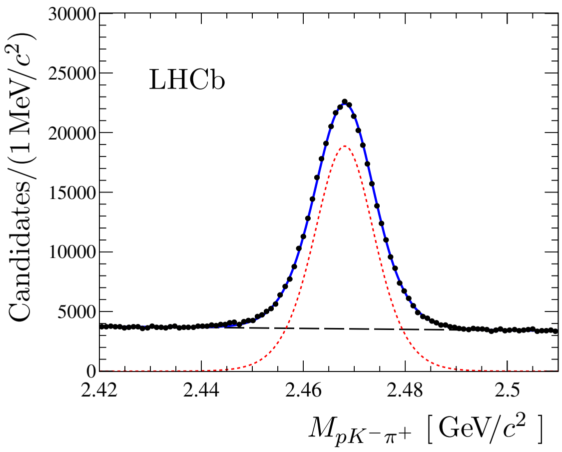

Figure 3. Fit results for the $\Xi_c^+ \to pK^-\pi^+$ decay. The red dotted line corresponds to the signal component, the black dashed line reflects the background distribution and the blue solid line is their sum.

where $\epsilon_{\rm acc}$ denotes the geometrical acceptance of the LHCb detector, $\epsilon_{\rm rec\&sel|acc}$ corresponds to the efficiency of reconstruction and selection of the candidates within the geometrical acceptance, $\epsilon_{\rm hardware|software}$ and $\epsilon_{\rm software|rec\&sel}$ are the trigger efficiencies for the selected candidates of the hardware and software levels, respectively, and $\epsilon_{\rm PID}$ is the PID efficiency. Since the hardware trigger level accepts events independently of the reconstructed candidates, *i.e.* the events belong to the TIS category, the efficiency $\epsilon_{\rm hardware|software}$ is assumed to cancel in the ratio of the signal and normalisation efficiencies. All other efficiencies except $\epsilon_{\rm PID}$ are determined from simulation. The simulated sample of $\Xi_c^+ \to pK^-K^+$ events with the intermediate ϕ resonance is used to determine efficiencies for the signal decay channel. The simulated sample for the $\Xi_c^+ \to pK^-\pi^+$ decay was produced according to a phase-space distribution. It is corrected to reproduce the Dalitz plot distribution observed with data. An additional correction is introduced for both simulated samples to account for the difference in the tracking efficiencies between data and simulation [35].

The PID efficiencies for the hadrons are determined from large samples of protons, kaons, and pions [27]. These samples are binned in momentum and pseudorapidity of the hadron, as well as in the charged particle multiplicity of the event. The PID efficiency for the Ξ_c^+ candidates are determined on an event-by-event basis. The weights for each candidate are taken from the calibration histograms using trilinear interpolation. The efficiency $\epsilon_{\rm PID}$ is determined as the ratio of Ξ_c^+ yields obtained from maximum-likelihood fits of the $M_{pK^-h^+}$ distributions from the weighted and unweighted samples.

The ratio between the total efficiencies of the signal and the normalisation decay channels is determined in bins of $p_{\rm T}$ and y of the Ξ_c^+ baryon. This procedure accounts for kinematic features of the Ξ_c^+ production, which could be poorly modelled in the simulation. Averaged over the $(p_{\rm T}, y)$ bins this ratio is determined to be $(91.1 \pm 3.6)\%$, including systematic uncertainties.

To reduce the effect of the dependence of the efficiency on the Ξ_c^+ kinematics, the mass fits are repeated in seven nonoverlapping $(p_{\rm T}, y)$ bins, which cover the LHCb fiducial

JHEP04(2019)084

Source	Uncertainty (%)
Signal fit model	0.5
Background fit model	0.5
sPlot-related uncertainty	1.0
Trigger efficiency	3.0
PID efficiency	2.2
Tracking	1.0
(p_{T},y) binning	1.3
Size of simulation sample	0.7
Selection requirements	0.8
Total	4.4

Table 1. Systematic uncertainties relative to the central value of the ratio $R_{p\phi}$.

volume. The fit procedure is the same as described above, except that the σ parameter of the signal distribution in eq. (4.1) is fixed to the value of the normalisation decay channel, scaled by a factor obtained from a fit to the $\Lambda_c^+ \to pK^-K^+$ and $\Lambda_c^+ \to pK^-\pi^+$ mass distributions in the same (p_{T}, y) bins. The ratios of the yields of the signal and normalisation decay channels are corrected by the ratios of the total efficiencies. The branching fraction ratios are evaluated for each (p_{T}, y) bin as

$$R_{p\phi} = \frac{N_{pKK} f_\phi}{\mathcal{B}(\phi \to K^+K^-)} \times \frac{1}{N_{pK\pi}} \times \frac{\epsilon_{\mathrm{total}}^{pK\pi}}{\epsilon_{\mathrm{total}}^{p\phi}}. \tag{5.2}$$

The known value of $\mathcal{B}(\phi \to K^+K^-) = 0.492 \pm 0.005$ is used [4]. The weighted average of the branching fraction ratios evaluated for the (p_{T}, y) bins is $R_{p\phi} = (19.8 \pm 0.7) \times 10^{-3}$, where the uncertainty reflects the statistical uncertainty of the Ξ_c^+ yields and f_ϕ. The alternative two-dimensional fitting procedure gives $R_{p\phi} = (19.8 \pm 0.8) \times 10^{-3}$, which is in excellent agreement with the result determined using the *sPlot* technique.

6 Systematic uncertainties

The list of systematic uncertainties for the measured ratio $R_{p\phi}$ is presented in table 1. The total uncertainty is obtained as the quadratic sum of all contributions.

In order to estimate the systematic uncertainties for the yields of the $\Xi_c^+ \to pK^-K^+$ and the normalisation decay channels, various hypotheses are tested for the description of the signal and background shapes. When the signal parameterisations in the $M_{pK^-K^+}$ and $M_{pK^-\pi^+}$ spectra are changed to a modified Novosibirsk function [36], no significant deviation from the nominal fit model is found. The change of the function for the non-ϕ component to a two-body phase space model in the fit to the $M_{K^-K^+}$ distribution leads to a systematic uncertainty of 0.5%, which is considered as the signal fit-model uncertainty.

The background-model parameterisation is tested by replacing of polynomial function with a product of polynomial and exponential functions. The uncertainty related to the *sPlot* method is studied with two samples of 500 pseudoexperiments each, in which the

JHEP04(2019)084

samples are generated according to the $M_{pK^-K^+}$–$M_{K^-K^+}$ model described in section 4. In one set of pseudoexperiments the effect of the residual correlation between $M_{pK^-K^+}$ and $M_{K^-K^+}$ is introduced. The systematic uncertainty of the *sPlot* technique is assigned from the deviations of the results of these tests from the nominal ones.

The cancellation of the hardware-trigger efficiencies in the ratio of the signal and the normalisation decay channels is studied with the Λ_c^+ control samples. A technique based on the partial overlap of the TIS and TOS subsamples [18] is used to evaluate hardware efficiencies for the $\Lambda_c^+ \to pK^-h^+$ decay channels. The data are consistent with the hypothesis of equal hardware-trigger efficiencies for the signal and normalisation decay channels. The precision achieved by means of these studies, limited by the statistics in the overlap between the TIS and TOS subsamples, is used as a systematic uncertainty for the hardware-trigger efficiency ratio.

For the software-trigger, the systematic uncertainty is assessed using simulation. The large variation of software-trigger requirements demonstrates the stability of the ratio of software-trigger efficiencies for the signal and normalisation decay channels at the 1% to 2% level. The overall systematic uncertainty for both hardware- and software-trigger efficiencies is dominated by the former and is reported in table 1.

The main source of uncertainty of the PID efficiency is related to the difference between results obtained with different calibration samples for the protons. The $\Lambda_c^+ \to pK^-\pi^+$ sample is used as default in the analysis, while results obtained with the $\Lambda \to p\pi^-$ calibration sample are used to assign a systematic uncertainty. For determination of PID efficiencies the calibration samples are binned according to proton, pion, or kaon kinematics. The associated systematic uncertainty is studied by comparing the results with different binning and interpolation schemes. The uncertainty related to the finite size of the calibration samples is considered to be fully correlated between the signal and normalisation decay channels and to cancel in the ratio.

The dominant uncertainty on the tracking efficiency correction arises from the different track reconstruction efficiency for kaons and pions due to different hadronic cross-sections with the detector material. Half of the $K^-\pi^+$ detection asymmetry measured by LHCb [37] is assigned as systematic uncertainty. Another source of uncertainty due to tracking efficiency is related to the binning of the tracking correction histogram. The difference between the results using interpolated and binned values of the efficiency is assigned as systematic uncertainty.

The uncertainty due to the selected (p_{T}, y)-bins to determine $R_{p\phi}$ is obtained from studies carried out with an alternative binning. There is an uncertainty of 0.7% from the size of the simulation sample. The obtained value of $R_{p\phi}$ is stable within 0.8% against a variation of selection requirements. This value is taken as the uncertainty due to the selection requirements. The uncertainty related to the Dalitz plot correction procedure applied to the simulated sample is estimated by a variation of the $R_{p\phi}$ ratio obtained with different binnings of the histogram used for this correction. This uncertainty is found to be small with respect to other sources of uncertainty.

JHEP04(2019)084

7 Conclusions

The first observation of the DCS $\Xi_c^+ \to p\phi$ decay is presented, using pp collision data collected with the LHCb detector at a centre-of-mass energy of 8 TeV, corresponding to an integrated luminosity of 2 fb^{-1}. The ratio of the branching fractions with respect to the SCS $\Xi_c^+ \to pK^-\pi^+$ decay channel is measured to be

$$R_{p\phi} = (19.8 \pm 0.7 \pm 0.9 \pm 0.2) \times 10^{-3},$$

where the first uncertainty is statistical, the second systematic and the third due to the knowledge of the $\phi \to K^+K^-$ branching fraction. An evidence of the 3.5σ, including systematic uncertainties, for a non-ϕ contribution to the DCS $\Xi_c^+ \to pK^-K^+$ decay is also found.

Acknowledgments

We express our gratitude to our colleagues in the CERN accelerator departments for the excellent performance of the LHC. We thank the technical and administrative staff at the LHCb institutes. We acknowledge support from CERN and from the national agencies: CAPES, CNPq, FAPERJ and FINEP (Brazil); MOST and NSFC (China); CNRS/IN2P3 (France); BMBF, DFG and MPG (Germany); INFN (Italy); NWO (Netherlands); MNiSW and NCN (Poland); MEN/IFA (Romania); MSHE (Russia); MinECo (Spain); SNSF and SER (Switzerland); NASU (Ukraine); STFC (United Kingdom); NSF (U.S.A.). We acknowledge the computing resources that are provided by CERN, IN2P3 (France), KIT and DESY (Germany), INFN (Italy), SURF (Netherlands), PIC (Spain), GridPP (United Kingdom), RRCKI and Yandex LLC (Russia), CSCS (Switzerland), IFIN-HH (Romania), CBPF (Brazil), PL-GRID (Poland) and OSC (U.S.A.). We are indebted to the communities behind the multiple open-source software packages on which we depend. Individual groups or members have received support from AvH Foundation (Germany); EPLANET, Marie Skłodowska-Curie Actions and ERC (European Union); ANR, Labex P2IO and OCEVU, and Région Auvergne-Rhône-Alpes (France); Key Research Program of Frontier Sciences of CAS, CAS PIFI, and the Thousand Talents Program (China); RFBR, RSF and Yandex LLC (Russia); GVA, XuntaGal and GENCAT (Spain); the Royal Society and the Leverhulme Trust (United Kingdom); Laboratory Directed Research and Development program of LANL (U.S.A.).

References

[1] N. Cabibbo, *Unitary symmetry and leptonic decays*, *Phys. Rev. Lett.* **10** (1963) 531 [INSPIRE].

[2] M. Kobayashi and T. Maskawa, *CP violation in the renormalizable theory of weak interaction*, *Prog. Theor. Phys.* **49** (1973) 652 [INSPIRE].

JHEP04(2019)084

[3] L. Wolfenstein, *Parametrization of the Kobayashi-Maskawa matrix*, Phys. Rev. Lett. **51** (1983) 1945 [INSPIRE].

[4] PARTICLE DATA GROUP collaboration, *Review of particle physics*, Phys. Rev. **D 98** (2018) 030001 [INSPIRE].

[5] K.K. Sharma and R.C. Verma, SU(3) *flavor analysis of two-body weak decays of charmed baryons*, Phys. Rev. **D 55** (1997) 7067 [hep-ph/9704391] [INSPIRE].

[6] S. Bianco, F.L. Fabbri, D. Benson and I. Bigi, *A Cicerone for the physics of charm*, Riv. Nuovo Cim. **26N7** (2003) 1 [hep-ex/0309021] [INSPIRE].

[7] B. Blok and M.A. Shifman, *Lifetimes of charmed hadrons revisited. Facts and fancy*, in the proceedings of the 3rd *workshop Tau charm factory*, June 1–6, Marbella, Spain (1993), hep-ph/9311331 [INSPIRE].

[8] H.-Y. Cheng, *Charmed baryons circa 2015*, arXiv:1508.07233 [INSPIRE].

[9] LHCb collaboration, *Measurement of the Ω_c^0 baryon lifetime*, Phys. Rev. Lett. **121** (2018) 092003 [arXiv:1807.02024] [INSPIRE].

[10] BELLE collaboration, *First observation of doubly cabibbo-suppressed decay of a charmed baryon: $\Lambda_c^+ \to pK^+\pi^-$*, Phys. Rev. Lett. **117** (2016) 011801 [arXiv:1512.07366] [INSPIRE].

[11] LHCb collaboration, *Measurements of the branching fractions of $\Lambda_c^+ \to p\pi^-\pi^+$, $\Lambda_c^+ \to pK^-K^+$ and $\Lambda_c^+ \to p\pi^-K^+$*, JHEP **03** (2018) 043 [arXiv:1711.01157] [INSPIRE].

[12] LHCb collaboration, *The LHCb detector at the LHC*, 2008 JINST **3** S08005 [INSPIRE].

[13] LHCb collaboration, *LHCb detector performance*, Int. J. Mod. Phys. **A 30** (2015) 1530022 [arXiv:1412.6352] [INSPIRE].

[14] R. Aaij et al., *Performance of the LHCb vertex locator*, 2014 JINST **9** P09007 [arXiv:1405.7808] [INSPIRE].

[15] R. Arink et al., *Performance of the LHCb outer tracker*, 2014 JINST **9** P01002 [arXiv:1311.3893] [INSPIRE].

[16] M. Adinolfi et al., *Performance of the LHCb RICH detector at the LHC*, Eur. Phys. J. **C 73** (2013) 2431 [arXiv:1211.6759] [INSPIRE].

[17] A.A. Alves Jr. et al., *Performance of the LHCb muon system*, 2013 JINST **8** P02022 [arXiv:1211.1346] [INSPIRE].

[18] R. Aaij et al., *The LHCb Trigger and its Performance in 2011*, 2013 JINST **8** P04022 [arXiv:1211.3055] [INSPIRE].

[19] T. Sjöstrand, S. Mrenna and P.Z. Skands, *PYTHIA 6.4 physics and manual*, JHEP **05** (2006) 026 [hep-ph/0603175] [INSPIRE].

[20] T. Sjöstrand, S. Mrenna and P.Z. Skands, *A brief introduction to PYTHIA 8.1*, Comput. Phys. Commun. **178** (2008) 852 [arXiv:0710.3820] [INSPIRE].

[21] I. Belyaev et al., *Handling of the generation of primary events in Gauss, the LHCb simulation framework*, J. Phys. Conf. Ser. **331** (2011) 032047 [INSPIRE].

[22] D.J. Lange, *The EvtGen particle decay simulation package*, Nucl. Instrum. Meth. **A 462** (2001) 152 [INSPIRE].

[23] P. Golonka and Z. Was, *PHOTOS Monte Carlo: a precision tool for QED corrections in Z and W decays*, Eur. Phys. J. **C 45** (2006) 97 [hep-ph/0506026] [INSPIRE].

JHEP04(2019)084

[24] GEANT4 collaboration, *GEANT4 developments and applications*, *IEEE Trans. Nucl. Sci.* **53** (2006) 270.

[25] GEANT4 collaboration, *GEANT4 — A simulation toolkit*, *Nucl. Instrum. Meth.* **A 506** (2003) 250 [INSPIRE].

[26] M. Clemencic et al., *The LHCb simulation application, Gauss: design, evolution and experience*, *J. Phys. Conf. Ser.* **331** (2011) 032023 [INSPIRE].

[27] L. Anderlini et al., *The PIDCalib package*, LHCb-PUB-2016-021 (2016).

[28] W.D. Hulsbergen, *Decay chain fitting with a Kalman filter*, *Nucl. Instrum. Meth.* **A 552** (2005) 566 [physics/0503191] [INSPIRE].

[29] I. Belyaev, A. Mazurov, T. Ovsiannikova and E. Rodrigues, *Ostap project*, available on Zenodo (2018).

[30] M. Pivk and F.R. Le Diberder, *SPlot: a statistical tool to unfold data distributions*, *Nucl. Instrum. Meth.* **A 555** (2005) 356 [physics/0402083] [INSPIRE].

[31] F. Von Hippel and C. Quigg, *Centrifugal-barrier effects in resonance partial decay widths, shapes and production amplitudes*, *Phys. Rev.* **D 5** (1972) 624 [INSPIRE].

[32] S.M. Flatte, *Coupled-channel analysis of the $\pi\eta$ and $K\bar{K}$ systems near $K\bar{K}$ threshold*, *Phys. Lett.* **63B** (1976) 224 [INSPIRE].

[33] BES collaboration, *Resonances in $J/\psi \to \phi\pi^+\pi^-$ and ϕK^+K^-*, *Phys. Lett.* **B 607** (2005) 243 [hep-ex/0411001] [INSPIRE].

[34] S.S. Wilks, *The large-sample distribution of the likelihood ratio for testing composite hypotheses*, *Annals Math. Statist.* **9** (1938) 60 [INSPIRE].

[35] LHCb collaboration, *Measurement of the track reconstruction efficiency at LHCb*, 2015 *JINST* **10** P02007 [arXiv:1408.1251] [INSPIRE].

[36] BABAR collaboration, *Branching fraction measurements of the color-suppressed decays $\bar{B}^0 \to D^{(*)0}\pi^0$, $D^{(*)0}\eta$, $D^{(*)0}\omega$ and $D^{(*)0}\eta'$ and measurement of the polarization in the decay $\bar{B}^0 \to D^{*0}\omega$*, *Phys. Rev.* **D 84** (2011) 112007 [*Erratum ibid.* **D 87** (2013) 039901] [arXiv:1107.5751] [INSPIRE].

[37] LHCb collaboration, *Measurement of CP asymmetry in $D^0 \to K^-K^+$ and $D^0 \to \pi^-\pi^+$ decays*, *JHEP* **07** (2014) 041 [arXiv:1405.2797] [INSPIRE].

The LHCb collaboration

R. Aaij[28], C. Abellán Beteta[46], B. Adeva[43], M. Adinolfi[50], C.A. Aidala[78], Z. Ajaltouni[6], S. Akar[61], P. Albicocco[19], J. Albrecht[11], F. Alessio[44], M. Alexander[55], A. Alfonso Albero[42], G. Alkhazov[34], P. Alvarez Cartelle[57], A.A. Alves Jr[43], S. Amato[2], S. Amerio[24], Y. Amhis[8], L. An[3], L. Anderlini[18], G. Andreassi[45], M. Andreotti[17], J.E. Andrews[62], F. Archilli[28], P. d'Argent[13], J. Arnau Romeu[7], A. Artamonov[41], M. Artuso[63], K. Arzymatov[38], E. Aslanides[7], M. Atzeni[46], B. Audurier[23], S. Bachmann[13], J.J. Back[52], S. Baker[57], V. Balagura[8,b], W. Baldini[17], A. Baranov[38], R.J. Barlow[58], G.C. Barrand[8], S. Barsuk[8], W. Barter[58], M. Bartolini[20], F. Baryshnikov[74], V. Batozskaya[32], B. Batsukh[63], A. Battig[11], V. Battista[45], A. Bay[45], J. Beddow[55], F. Bedeschi[25], I. Bediaga[1], A. Beiter[63], L.J. Bel[28], S. Belin[23], N. Beliy[66], V. Bellee[45], N. Belloli[21,i], K. Belous[41], I. Belyaev[35], E. Ben-Haim[9], G. Bencivenni[19], S. Benson[28], S. Beranek[10], A. Berezhnoy[36], R. Bernet[46], D. Berninghoff[13], E. Bertholet[9], A. Bertolin[24], C. Betancourt[46], F. Betti[16,44], M.O. Bettler[51], M. van Beuzekom[28], Ia. Bezshyiko[46], S. Bhasin[50], J. Bhom[30], S. Bifani[49], P. Billoir[9], A. Birnkraut[11], A. Bizzeti[18,u], M. Bjørn[59], M.P. Blago[44], T. Blake[52], F. Blanc[45], S. Blusk[63], D. Bobulska[55], V. Bocci[27], O. Boente Garcia[43], T. Boettcher[60], A. Bondar[40,x], N. Bondar[34], S. Borghi[58,44], M. Borisyak[38], M. Borsato[43], F. Bossu[8], M. Boubdir[10], T.J.V. Bowcock[56], C. Bozzi[17,44], S. Braun[13], M. Brodski[44], J. Brodzicka[30], A. Brossa Gonzalo[52], D. Brundu[23,44], E. Buchanan[50], A. Buonaura[46], C. Burr[58], A. Bursche[23], J. Buytaert[44], W. Byczynski[44], S. Cadeddu[23], H. Cai[68], R. Calabrese[17,g], R. Calladine[49], M. Calvi[21,i], M. Calvo Gomez[42,m], A. Camboni[42,m], P. Campana[19], D.H. Campora Perez[44], L. Capriotti[16], A. Carbone[16,e], G. Carboni[26], R. Cardinale[20], A. Cardini[23], P. Carniti[21,i], L. Carson[54], K. Carvalho Akiba[2], G. Casse[56], L. Cassina[21], M. Cattaneo[44], G. Cavallero[20], R. Cenci[25,p], D. Chamont[8], M.G. Chapman[50], M. Charles[9], Ph. Charpentier[44], G. Chatzikonstantinidis[49], M. Chefdeville[5], V. Chekalina[38], C. Chen[3], S. Chen[23], S.-G. Chitic[44], V. Chobanova[43], M. Chrzaszcz[44], A. Chubykin[34], P. Ciambrone[19], X. Cid Vidal[43], G. Ciezarek[44], F. Cindolo[16], P.E.L. Clarke[54], M. Clemencic[44], H.V. Cliff[51], J. Closier[44], V. Coco[44], J.A.B. Coelho[8], J. Cogan[7], E. Cogneras[6], L. Cojocariu[33], P. Collins[44], T. Colombo[44], A. Comerma-Montells[13], A. Contu[23], G. Coombs[44], S. Coquereau[42], G. Corti[44], M. Corvo[17,g], C.M. Costa Sobral[52], B. Couturier[44], G.A. Cowan[54], D.C. Craik[60], A. Crocombe[52], M. Cruz Torres[1], R. Currie[54], C. D'Ambrosio[44], F. Da Cunha Marinho[2], C.L. Da Silva[79], E. Dall'Occo[28], J. Dalseno[43,v], A. Danilina[35], A. Davis[3], O. De Aguiar Francisco[44], K. De Bruyn[44], S. De Capua[58], M. De Cian[45], J.M. De Miranda[1], L. De Paula[2], M. De Serio[15,d], P. De Simone[19], C.T. Dean[55], D. Decamp[5], L. Del Buono[9], B. Delaney[51], H.-P. Dembinski[12], M. Demmer[11], A. Dendek[31], D. Derkach[39], O. Deschamps[6], F. Desse[8], F. Dettori[56], B. Dey[69], A. Di Canto[44], P. Di Nezza[19], S. Didenko[74], H. Dijkstra[44], F. Dordei[44], M. Dorigo[44,y], A. Dosil Suárez[43], L. Douglas[55], A. Dovbnya[47], K. Dreimanis[56], L. Dufour[28], G. Dujany[9], P. Durante[44], J.M. Durham[79], D. Dutta[58], R. Dzhelyadin[41], M. Dziewiecki[13], A. Dziurda[30], A. Dzyuba[34], S. Easo[53], U. Egede[57], V. Egorychev[35], S. Eidelman[40,x], S. Eisenhardt[54], U. Eitschberger[11], R. Ekelhof[11], L. Eklund[55], S. Ely[63], A. Ene[33], S. Escher[10], S. Esen[28], T. Evans[61], A. Falabella[16], N. Farley[49], S. Farry[56], D. Fazzini[21,44,i], L. Federici[26], P. Fernandez Declara[44], A. Fernandez Prieto[43], F. Ferrari[16], L. Ferreira Lopes[45], F. Ferreira Rodrigues[2], M. Ferro-Luzzi[44], S. Filippov[37], R.A. Fini[15], M. Fiorini[17,g], M. Firlej[31], C. Fitzpatrick[45], T. Fiutowski[31], F. Fleuret[8,b], M. Fontana[44], F. Fontanelli[20,h], R. Forty[44], V. Franco Lima[56], M. Frank[44], C. Frei[44], J. Fu[22,q], W. Funk[44], C. Färber[44], M. Féo[28], E. Gabriel[54], A. Gallas Torreira[43], D. Galli[16,e], S. Gallorini[24], S. Gambetta[54], Y. Gan[3], M. Gandelman[2], P. Gandini[22], Y. Gao[3], L.M. Garcia Martin[76], B. Garcia Plana[43], J. García Pardiñas[46], J. Garra Tico[51], L. Garrido[42], D. Gascon[42], C. Gaspar[44], L. Gavardi[11],

G. Gazzoni[6], D. Gerick[13], E. Gersabeck[58], M. Gersabeck[58], T. Gershon[52], D. Gerstel[7], Ph. Ghez[5], V. Gibson[51], O.G. Girard[45], P. Gironella Gironell[42], L. Giubega[33], K. Gizdov[54], V.V. Gligorov[9], D. Golubkov[35], A. Golutvin[57,74], A. Gomes[1,a], I.V. Gorelov[36], C. Gotti[21,i], E. Govorkova[28], J.P. Grabowski[13], R. Graciani Diaz[42], L.A. Granado Cardoso[44], E. Graugés[42], E. Graverini[46], G. Graziani[18], A. Grecu[33], R. Greim[28], P. Griffith[23], L. Grillo[58], L. Gruber[44], B.R. Gruberg Cazon[59], O. Grünberg[71], C. Gu[3], E. Gushchin[37], A. Guth[10], Yu. Guz[41,44], T. Gys[44], C. Göbel[65], T. Hadavizadeh[59], C. Hadjivasiliou[6], G. Haefeli[45], C. Haen[44], S.C. Haines[51], B. Hamilton[62], X. Han[13], T.H. Hancock[59], S. Hansmann-Menzemer[13], N. Harnew[59], S.T. Harnew[50], T. Harrison[56], C. Hasse[44], M. Hatch[44], J. He[66], M. Hecker[57], K. Heinicke[11], A. Heister[11], K. Hennessy[56], L. Henry[76], E. van Herwijnen[44], J. Heuel[10], M. Heß[71], A. Hicheur[64], R. Hidalgo Charman[58], D. Hill[59], M. Hilton[58], P.H. Hopchev[45], J. Hu[13], W. Hu[69], W. Huang[66], Z.C. Huard[61], W. Hulsbergen[28], T. Humair[57], M. Hushchyn[39], D. Hutchcroft[56], D. Hynds[28], P. Ibis[11], M. Idzik[31], P. Ilten[49], A. Inglessi[34], A. Inyakin[41], K. Ivshin[34], R. Jacobsson[44], J. Jalocha[59], E. Jans[28], B.K. Jashal[76], A. Jawahery[62], F. Jiang[3], M. John[59], D. Johnson[44], C.R. Jones[51], C. Joram[44], B. Jost[44], N. Jurik[59], S. Kandybei[47], M. Karacson[44], J.M. Kariuki[50], S. Karodia[55], N. Kazeev[39], M. Kecke[13], F. Keizer[51], M. Kelsey[63], M. Kenzie[51], T. Ketel[29], E. Khairullin[38], B. Khanji[44], C. Khurewathanakul[45], K.E. Kim[63], T. Kirn[10], S. Klaver[19], K. Klimaszewski[32], T. Klimkovich[12], S. Koliiev[48], M. Kolpin[13], R. Kopecna[13], P. Koppenburg[28], I. Kostiuk[28], S. Kotriakhova[34], M. Kozeiha[6], L. Kravchuk[37], M. Kreps[52], F. Kress[57], P. Krokovny[40,x], W. Krupa[31], W. Krzemien[32], W. Kucewicz[30,l], M. Kucharczyk[30], V. Kudryavtsev[40,x], A.K. Kuonen[45], T. Kvaratskheliya[35,44], D. Lacarrere[44], G. Lafferty[58], A. Lai[23], D. Lancierini[46], G. Lanfranchi[19], C. Langenbruch[10], T. Latham[52], C. Lazzeroni[49], R. Le Gac[7], A. Leflat[36], J. Lefrançois[8], R. Lefèvre[6], F. Lemaitre[44], O. Leroy[7], T. Lesiak[30], B. Leverington[13], P.-R. Li[66,ab], Y. Li[4], Z. Li[63], X. Liang[63], T. Likhomanenko[73], R. Lindner[44], F. Lionetto[46], V. Lisovskyi[8], G. Liu[67], X. Liu[3], D. Loh[52], A. Loi[23], I. Longstaff[55], J.H. Lopes[2], G.H. Lovell[51], D. Lucchesi[24,o], M. Lucio Martinez[43], A. Lupato[24], E. Luppi[17,g], O. Lupton[44], A. Lusiani[25], X. Lyu[66], F. Machefert[8], F. Maciuc[33], V. Macko[45], P. Mackowiak[11], S. Maddrell-Mander[50], O. Maev[34,44], K. Maguire[58], D. Maisuzenko[34], M.W. Majewski[31], S. Malde[59], B. Malecki[30], A. Malinin[73], T. Maltsev[40,x], G. Manca[23,f], G. Mancinelli[7], D. Marangotto[22,q], J. Maratas[6,w], J.F. Marchand[5], U. Marconi[16], C. Marin Benito[8], M. Marinangeli[45], P. Marino[45], J. Marks[13], P.J. Marshall[56], G. Martellotti[27], M. Martin[7], M. Martinelli[44], D. Martinez Santos[43], F. Martinez Vidal[76], A. Massafferri[1], M. Materok[10], R. Matev[44], A. Mathad[52], Z. Mathe[44], C. Matteuzzi[21], A. Mauri[46], E. Maurice[8,b], B. Maurin[45], A. Mazurov[49], M. McCann[57,44], A. McNab[58], R. McNulty[14], J.V. Mead[56], B. Meadows[61], C. Meaux[7], N. Meinert[71], D. Melnychuk[32], M. Merk[28], A. Merli[22,q], E. Michielin[24], D.A. Milanes[70], E. Millard[52], M.-N. Minard[5], L. Minzoni[17,g], D.S. Mitzel[13], A. Mogini[9], R.D. Moise[57], T. Mombächer[11], I.A. Monroy[70], S. Monteil[6], M. Morandin[24], G. Morello[19], M.J. Morello[25,t], O. Morgunova[73], J. Moron[31], A.B. Morris[7], R. Mountain[63], F. Muheim[54], M. Mukherjee[69], M. Mulder[28], C.H. Murphy[59], D. Murray[58], A. Mödden [11], D. Müller[44], J. Müller[11], K. Müller[46], V. Müller[11], P. Naik[50], T. Nakada[45], R. Nandakumar[53], A. Nandi[59], T. Nanut[45], I. Nasteva[2], M. Needham[54], N. Neri[22,q], S. Neubert[13], N. Neufeld[44], M. Neuner[13], R. Newcombe[57], T.D. Nguyen[45], C. Nguyen-Mau[45,n], S. Nieswand[10], R. Niet[11], N. Nikitin[36], A. Nogay[73], N.S. Nolte[44], D.P. O'Hanlon[16], A. Oblakowska-Mucha[31], V. Obraztsov[41], S. Ogilvy[55], R. Oldeman[23,f], C.J.G. Onderwater[72], A. Ossowska[30], J.M. Otalora Goicochea[2], T. Ovsiannikova[35], P. Owen[46], A. Oyanguren[76], P.R. Pais[45], T. Pajero[25,t], A. Palano[15], M. Palutan[19], G. Panshin[75], A. Papanestis[53], M. Pappagallo[54], L.L. Pappalardo[17,g], W. Parker[62], C. Parkes[58,44], G. Passaleva[18,44], A. Pastore[15], M. Patel[57], C. Patrignani[16,e], A. Pearce[44], A. Pellegrino[28], G. Penso[27], M. Pepe Altarelli[44], S. Perazzini[44], D. Pereima[35], P. Perret[6],

L. Pescatore[45], K. Petridis[50], A. Petrolini[20,h], A. Petrov[73], S. Petrucci[54], M. Petruzzo[22,q], B. Pietrzyk[5], G. Pietrzyk[45], M. Pikies[30], M. Pili[59], D. Pinci[27], J. Pinzino[44], F. Pisani[44], A. Piucci[13], V. Placinta[33], S. Playfer[54], J. Plews[49], M. Plo Casasus[43], F. Polci[9], M. Poli Lener[19], A. Poluektov[52], N. Polukhina[74,c], I. Polyakov[63], E. Polycarpo[2], G.J. Pomery[50], S. Ponce[44], A. Popov[41], D. Popov[49,12], S. Poslavskii[41], E. Price[50], J. Prisciandaro[43], C. Prouve[50], V. Pugatch[48], A. Puig Navarro[46], H. Pullen[59], G. Punzi[25,p], W. Qian[66], J. Qin[66], R. Quagliani[9], B. Quintana[6], N.V. Raab[14], B. Rachwal[31], J.H. Rademacker[50], M. Rama[25], M. Ramos Pernas[43], M.S. Rangel[2], F. Ratnikov[38,39], G. Raven[29], M. Ravonel Salzgeber[44], M. Reboud[5], F. Redi[45], S. Reichert[11], A.C. dos Reis[1], F. Reiss[9], C. Remon Alepuz[76], Z. Ren[3], V. Renaudin[8], S. Ricciardi[53], S. Richards[50], K. Rinnert[56], P. Robbe[8], A. Robert[9], A.B. Rodrigues[45], E. Rodrigues[61], J.A. Rodriguez Lopez[70], M. Roehrken[44], S. Roiser[44], A. Rollings[59], V. Romanovskiy[41], A. Romero Vidal[43], M. Rotondo[19], M.S. Rudolph[63], T. Ruf[44], J. Ruiz Vidal[76], J.J. Saborido Silva[43], N. Sagidova[34], B. Saitta[23,f], V. Salustino Guimaraes[65], C. Sanchez Gras[28], C. Sanchez Mayordomo[76], B. Sanmartin Sedes[43], R. Santacesaria[27], C. Santamarina Rios[43], M. Santimaria[19,44], E. Santovetti[26,j], G. Sarpis[58], A. Sarti[19,k], C. Satriano[27,s], A. Satta[26], M. Saur[66], D. Savrina[35,36], S. Schael[10], M. Schellenberg[11], M. Schiller[55], H. Schindler[44], M. Schmelling[12], T. Schmelzer[11], B. Schmidt[44], O. Schneider[45], A. Schopper[44], H.F. Schreiner[61], M. Schubiger[45], S. Schulte[45], M.H. Schune[8], R. Schwemmer[44], B. Sciascia[19], A. Sciubba[27,k], A. Semennikov[35], E.S. Sepulveda[9], A. Sergi[49], N. Serra[46], J. Serrano[7], L. Sestini[24], A. Seuthe[11], P. Seyfert[44], M. Shapkin[41], Y. Shcheglov[34,†], T. Shears[56], L. Shekhtman[40,x], V. Shevchenko[73], E. Shmanin[74], B.G. Siddi[17], R. Silva Coutinho[46], L. Silva de Oliveira[2], G. Simi[24,o], S. Simone[15,d], I. Skiba[17], N. Skidmore[13], T. Skwarnicki[63], M.W. Slater[49], J.G. Smeaton[51], E. Smith[10], I.T. Smith[54], M. Smith[57], M. Soares[16], l. Soares Lavra[1], M.D. Sokoloff[61], F.J.P. Soler[55], B. Souza De Paula[2], B. Spaan[11], E. Spadaro Norella[22,q], P. Spradlin[55], F. Stagni[44], M. Stahl[13], S. Stahl[44], P. Stefko[45], S. Stefkova[57], O. Steinkamp[46], S. Stemmle[13], O. Stenyakin[41], M. Stepanova[34], H. Stevens[11], A. Stocchi[8], S. Stone[63], B. Storaci[46], S. Stracka[25], M.E. Stramaglia[45], M. Straticiuc[33], U. Straumann[46], S. Strokov[75], J. Sun[3], L. Sun[68], Y. Sun[62], K. Swientek[31], A. Szabelski[32], T. Szumlak[31], M. Szymanski[66], S. T'Jampens[5], Z. Tang[3], A. Tayduganov[7], T. Tekampe[11], G. Tellarini[17], F. Teubert[44], E. Thomas[44], J. van Tilburg[28], M.J. Tilley[57], V. Tisserand[6], M. Tobin[31], S. Tolk[44], L. Tomassetti[17,g], D. Tonelli[25], D.Y. Tou[9], R. Tourinho Jadallah Aoude[1], E. Tournefier[5], M. Traill[55], M.T. Tran[45], A. Trisovic[51], A. Tsaregorodtsev[7], G. Tuci[25,p], A. Tully[51], N. Tuning[28,44], A. Ukleja[32], A. Usachov[8], A. Ustyuzhanin[38,39], U. Uwer[13], A. Vagner[75], V. Vagnoni[16], A. Valassi[44], S. Valat[44], G. Valenti[16], R. Vazquez Gomez[44], P. Vazquez Regueiro[43], S. Vecchi[17], M. van Veghel[28], J.J. Velthuis[50], M. Veltri[18,r], G. Veneziano[59], A. Venkateswaran[63], M. Vernet[6], M. Veronesi[28], M. Vesterinen[59], J.V. Viana Barbosa[44], D. Vieira[66], M. Vieites Diaz[43], H. Viemann[71], X. Vilasis-Cardona[42,m], A. Vitkovskiy[28], M. Vitti[51], V. Volkov[36], A. Vollhardt[46], D. Vom Bruch[9], B. Voneki[44], A. Vorobyev[34], V. Vorobyev[40,x], N. Voropaev[34], J.A. de Vries[28], C. Vázquez Sierra[28], R. Waldi[71], J. Walsh[25], J. Wang[4], M. Wang[3], Y. Wang[69], Z. Wang[46], D.R. Ward[51], H.M. Wark[56], N.K. Watson[49], D. Websdale[57], A. Weiden[46], C. Weisser[60], M. Whitehead[10], J. Wicht[52], G. Wilkinson[59], M. Wilkinson[63], I. Williams[51], M.R.J. Williams[58], M. Williams[60], T. Williams[49], F.F. Wilson[53], M. Winn[8], W. Wislicki[32], M. Witek[30], G. Wormser[8], S.A. Wotton[51], K. Wyllie[44], D. Xiao[69], Y. Xie[69], A. Xu[3], M. Xu[69], Q. Xu[66], Z. Xu[3], Z. Xu[5], Z. Yang[3], Z. Yang[62], Y. Yao[63], L.E. Yeomans[56], H. Yin[69], J. Yu[69,aa], X. Yuan[63], O. Yushchenko[41], K.A. Zarebski[49], M. Zavertyaev[12,c], D. Zhang[69], L. Zhang[3], W.C. Zhang[3,z], Y. Zhang[44], A. Zhelezov[13], Y. Zheng[66], X. Zhu[3], V. Zhukov[10,36], J.B. Zonneveld[54], S. Zucchelli[16]

[1] *Centro Brasileiro de Pesquisas Físicas (CBPF), Rio de Janeiro, Brazil*
[2] *Universidade Federal do Rio de Janeiro (UFRJ), Rio de Janeiro, Brazil*

[3] Center for High Energy Physics, Tsinghua University, Beijing, China
[4] Institute Of High Energy Physics (ihep), Beijing, China
[5] Univ. Grenoble Alpes, Univ. Savoie Mont Blanc, CNRS, IN2P3-LAPP, Annecy, France
[6] Université Clermont Auvergne, CNRS/IN2P3, LPC, Clermont-Ferrand, France
[7] Aix Marseille Univ, CNRS/IN2P3, CPPM, Marseille, France
[8] LAL, Univ. Paris-Sud, CNRS/IN2P3, Université Paris-Saclay, Orsay, France
[9] LPNHE, Sorbonne Université, Paris Diderot Sorbonne Paris Cité, CNRS/IN2P3, Paris, France
[10] I. Physikalisches Institut, RWTH Aachen University, Aachen, Germany
[11] Fakultät Physik, Technische Universität Dortmund, Dortmund, Germany
[12] Max-Planck-Institut für Kernphysik (MPIK), Heidelberg, Germany
[13] Physikalisches Institut, Ruprecht-Karls-Universität Heidelberg, Heidelberg, Germany
[14] School of Physics, University College Dublin, Dublin, Ireland
[15] INFN Sezione di Bari, Bari, Italy
[16] INFN Sezione di Bologna, Bologna, Italy
[17] INFN Sezione di Ferrara, Ferrara, Italy
[18] INFN Sezione di Firenze, Firenze, Italy
[19] INFN Laboratori Nazionali di Frascati, Frascati, Italy
[20] INFN Sezione di Genova, Genova, Italy
[21] INFN Sezione di Milano-Bicocca, Milano, Italy
[22] INFN Sezione di Milano, Milano, Italy
[23] INFN Sezione di Cagliari, Monserrato, Italy
[24] INFN Sezione di Padova, Padova, Italy
[25] INFN Sezione di Pisa, Pisa, Italy
[26] INFN Sezione di Roma Tor Vergata, Roma, Italy
[27] INFN Sezione di Roma La Sapienza, Roma, Italy
[28] Nikhef National Institute for Subatomic Physics, Amsterdam, Netherlands
[29] Nikhef National Institute for Subatomic Physics and VU University Amsterdam, Amsterdam, Netherlands
[30] Henryk Niewodniczanski Institute of Nuclear Physics Polish Academy of Sciences, Kraków, Poland
[31] AGH — University of Science and Technology, Faculty of Physics and Applied Computer Science, Kraków, Poland
[32] National Center for Nuclear Research (NCBJ), Warsaw, Poland
[33] Horia Hulubei National Institute of Physics and Nuclear Engineering, Bucharest-Magurele, Romania
[34] Petersburg Nuclear Physics Institute (PNPI), Gatchina, Russia
[35] Institute of Theoretical and Experimental Physics (ITEP), Moscow, Russia
[36] Institute of Nuclear Physics, Moscow State University (SINP MSU), Moscow, Russia
[37] Institute for Nuclear Research of the Russian Academy of Sciences (INR RAS), Moscow, Russia
[38] Yandex School of Data Analysis, Moscow, Russia
[39] National Research University Higher School of Economics, Moscow, Russia
[40] Budker Institute of Nuclear Physics (SB RAS), Novosibirsk, Russia
[41] Institute for High Energy Physics (IHEP), Protvino, Russia
[42] ICCUB, Universitat de Barcelona, Barcelona, Spain
[43] Instituto Galego de Física de Altas Enerxías (IGFAE), Universidade de Santiago de Compostela, Santiago de Compostela, Spain
[44] European Organization for Nuclear Research (CERN), Geneva, Switzerland
[45] Institute of Physics, Ecole Polytechnique Fédérale de Lausanne (EPFL), Lausanne, Switzerland
[46] Physik-Institut, Universität Zürich, Zürich, Switzerland
[47] NSC Kharkiv Institute of Physics and Technology (NSC KIPT), Kharkiv, Ukraine
[48] Institute for Nuclear Research of the National Academy of Sciences (KINR), Kyiv, Ukraine
[49] University of Birmingham, Birmingham, United Kingdom
[50] H.H. Wills Physics Laboratory, University of Bristol, Bristol, United Kingdom

JHEP04(2019)084

[51] Cavendish Laboratory, University of Cambridge, Cambridge, United Kingdom
[52] Department of Physics, University of Warwick, Coventry, United Kingdom
[53] STFC Rutherford Appleton Laboratory, Didcot, United Kingdom
[54] School of Physics and Astronomy, University of Edinburgh, Edinburgh, United Kingdom
[55] School of Physics and Astronomy, University of Glasgow, Glasgow, United Kingdom
[56] Oliver Lodge Laboratory, University of Liverpool, Liverpool, United Kingdom
[57] Imperial College London, London, United Kingdom
[58] School of Physics and Astronomy, University of Manchester, Manchester, United Kingdom
[59] Department of Physics, University of Oxford, Oxford, United Kingdom
[60] Massachusetts Institute of Technology, Cambridge, MA, United States
[61] University of Cincinnati, Cincinnati, OH, United States
[62] University of Maryland, College Park, MD, United States
[63] Syracuse University, Syracuse, NY, United States
[64] Laboratory of Mathematical and Subatomic Physics , Constantine, Algeria, associated to[2]
[65] Pontifícia Universidade Católica do Rio de Janeiro (PUC-Rio), Rio de Janeiro, Brazil, associated to[2]
[66] University of Chinese Academy of Sciences, Beijing, China, associated to[3]
[67] South China Normal University, Guangzhou, China, associated to[3]
[68] School of Physics and Technology, Wuhan University, Wuhan, China, associated to[3]
[69] Institute of Particle Physics, Central China Normal University, Wuhan, Hubei, China, associated to[3]
[70] Departamento de Fisica , Universidad Nacional de Colombia, Bogota, Colombia, associated to[9]
[71] Institut für Physik, Universität Rostock, Rostock, Germany, associated to[13]
[72] Van Swinderen Institute, University of Groningen, Groningen, Netherlands, associated to[28]
[73] National Research Centre Kurchatov Institute, Moscow, Russia, associated to[35]
[74] National University of Science and Technology "MISIS", Moscow, Russia, associated to[35]
[75] National Research Tomsk Polytechnic University, Tomsk, Russia, associated to[35]
[76] Instituto de Fisica Corpuscular, Centro Mixto Universidad de Valencia — CSIC, Valencia, Spain, associated to[42]
[77] H.H. Wills Physics Laboratory, University of Bristol, Bristol, United Kingdom, Bristol, United Kingdom
[78] University of Michigan, Ann Arbor, United States, associated to[63]
[79] Los Alamos National Laboratory (LANL), Los Alamos, United States, associated to[63]

[a] Universidade Federal do Triângulo Mineiro (UFTM), Uberaba-MG, Brazil
[b] Laboratoire Leprince-Ringuet, Palaiseau, France
[c] P.N. Lebedev Physical Institute, Russian Academy of Science (LPI RAS), Moscow, Russia
[d] Università di Bari, Bari, Italy
[e] Università di Bologna, Bologna, Italy
[f] Università di Cagliari, Cagliari, Italy
[g] Università di Ferrara, Ferrara, Italy
[h] Università di Genova, Genova, Italy
[i] Università di Milano Bicocca, Milano, Italy
[j] Università di Roma Tor Vergata, Roma, Italy
[k] Università di Roma La Sapienza, Roma, Italy
[l] AGH — University of Science and Technology, Faculty of Computer Science, Electronics and Telecommunications, Kraków, Poland
[m] LIFAELS, La Salle, Universitat Ramon Llull, Barcelona, Spain
[n] Hanoi University of Science, Hanoi, Vietnam
[o] Università di Padova, Padova, Italy
[p] Università di Pisa, Pisa, Italy
[q] Università degli Studi di Milano, Milano, Italy

JHEP04(2019)084

[r] Università di Urbino, Urbino, Italy
[s] Università della Basilicata, Potenza, Italy
[t] Scuola Normale Superiore, Pisa, Italy
[u] Università di Modena e Reggio Emilia, Modena, Italy
[v] H.H. Wills Physics Laboratory, University of Bristol, Bristol, United Kingdom
[w] MSU — Iligan Institute of Technology (MSU-IIT), Iligan, Philippines
[x] Novosibirsk State University, Novosibirsk, Russia
[y] Sezione INFN di Trieste, Trieste, Italy
[z] School of Physics and Information Technology, Shaanxi Normal University (SNNU), Xi'an, China
[aa] Physics and Micro Electronic College, Hunan University, Changsha City, China
[ab] Lanzhou University, Lanzhou, China
[†] Deceased

JHEP04(2019)084